Density-matrix renormalization-group study of the polaron problem in the Holstein model

Eric Jeckelmann and Steven R. White
Department of Physics and Astronomy, University of California, Irvine, California 92697
(Received 7 October 1997)

We propose a density-matrix renormalization-group (DMRG) approach to study lattices including bosons. The key to the approach is an exact mapping of a boson site containing 2^N states to N pseudosites, each with 2 states. The pseudosites can be viewed as the binary digits of a boson level. We apply the pseudosite DMRG method to the polaron problem in the one- and two-dimensional Holstein models. Ground-state results are presented for a wide range of electron-phonon coupling strengths and phonon frequencies on lattices large enough (up to 80 sites in one dimension and up to 20×20 sites in two dimensions) to eliminate finite-size effects, with up to 128 phonon states per phonon mode. We find a smooth but quite abrupt crossover from a quasi-free-electron ground state with a slightly renormalized mass at weak electron-phonon coupling to a polaronic ground state with a large effective mass at strong coupling, in agreement with previous studies. [S0163-1829(98)02112-2]

I. INTRODUCTION

The density-matrix renormalization-group (DMRG) method[1,2] has proved to be a very successful numerical technique for studying spin and fermion lattice models with short-range interactions in low dimensions. Although the DMRG algorithm can easily be generalized to treat systems including bosons, calculations are often not practical. As for exact diagonalizations, this is due to the difficulty in dealing with the large (in principle, infinite) dimension of the Hilbert space for bosons. Although the problem is less severe in DMRG than in exact diagonalizations, applications of DMRG to boson systems have been restricted to problems for which one needs to consider at most about a dozen states for each boson.[3–5]

In this paper, we present an approach for dealing with large bosonic Hilbert spaces with DMRG. The basic idea is to transform each boson site into several artificial interacting two-state sites (pseudosites) and then to use DMRG techniques to treat this interacting system. DMRG is much better able to handle several two-state sites rather than one many-state site. Although this procedure introduces some complications in a DMRG program, the pseudosite approach is more efficient and allows us to keep many more states in each bosonic Hilbert space than the approach used in earlier works.[3–5]

To test our method, we have studied the polaron problem, the self-trapping of an electron by a localized lattice deformation, in the Holstein model[6] in one and two dimensions. We consider a single electron on a lattice with oscillators of frequency ω at each site representing dispersionless optical phonon modes and a coupling between the electron density and oscillator displacements $q_\ell = b_\ell^\dagger + b_\ell$, where $b_\ell^\dagger$ and b_ℓ are the usual boson creation and annihilation operators. The Hamiltonian is given by

$$H = \omega \sum_\ell b_\ell^\dagger b_\ell - g\omega \sum_\ell (b_\ell^\dagger + b_\ell) n_\ell - t \sum_{\langle \ell, m\rangle} (c_m^\dagger c_\ell + c_\ell^\dagger c_m), \tag{1.1}$$

where $c_\ell^\dagger$ and c_ℓ are electron creation and annihilation operators, $n_\ell = c_\ell^\dagger c_\ell$, and t is the hopping integral. g is a dimensionless electron-phonon coupling constant. (When comparing results readers should be aware that notations for model parameters, especially g, differ in other papers.) A summation over ℓ or $\langle \ell, m\rangle$ means a sum over all sites or over all bonds between nearest-neighbor sites in a chain of length L or a square lattice of size $L\times L$. Only open systems have been considered because the DMRG method usually performs much better in this case than for periodic boundary conditions.

The polaron problem has been extensively studied using variational methods,[7] quantum Monte Carlo simulations,[8,9] exact diagonalizations,[10–14] and perturbation theory.[12,14,15] It is known that a rather sharp crossover occurs between a quasi-free-electron ground state with a slightly renormalized mass at weak electron-phonon coupling, and a polaronic ground state with a narrow bandwidth at strong coupling. However, despite these considerable theoretical efforts, the physics of this self-trapping transition is not fully understood. Previous studies have been limited either to small systems or to a particular regime of parameters g and ω/t or by a severely truncated phononic Hilbert space or by uncontrolled approximations. With the DMRG method, we have been able to study the one-electron ground state of the Holstein model for all regimes of parameters ω/t and g on large lattices and with great accuracy. In this work we report and discuss some ground state results that show the self-trapping crossover, such as electron-lattice displacement correlation functions, electronic kinetic energy, and effective mass.

This paper is organized as follows: in the next section, we present our pseudosite method for bosons. In Sec. III we describe how we apply this method to the Holstein model. Most results for the polaron problem are presented and discussed in Sec. IV. In Sec. V we explain how we have computed the effective mass of electrons and polarons and present these results. Finally, Sec. VI contains our conclusions.

II. DMRG FOR BOSON SYSTEMS

In the DMRG method, the lattice is broken up into blocks made of one or several sites and Hilbert spaces representing

blocks are truncated (for more details, see Refs. 1 and 2). In each block one keeps only the m most important states for forming the ground state (or low-energy eigenstates) of the full system. A step of the DMRG algorithm is the process of forming a new block by adding a site to a block obtained in a previous step. To find the m optimal states of the new enlarged block, one has to find the ground state of an effective Hamiltonian in a superblock made of two blocks and two sites and then to diagonalize a density matrix on the new block. If n is the number of states on a site, the computer memory storage needed to perform these tasks increases as n^2m^2, while the number of operations goes roughly as n^3m^3.

The difficulty in applying the DMRG to boson systems is the large number of states on a site. In principle, this number is infinite and for numerical calculations one has to truncate this space and keep a finite number M of states per boson. In a standard implementation of the DMRG method for boson systems, each boson forms one lattice site ($n\sim M$) and thus memory and CPU time requirements increase as M^2 and M^3, respectively. For many interesting problems, such as the Holstein polaron discussed in this paper, one needs to keep a large number of states per boson sites ($M\approx 10-100$) to reduce errors due to the truncation of bosonic Hilbert spaces. Therefore, performing such calculations requires much more computer resources than DMRG computations for otherwise similar Heisenberg or Hubbard systems, for which $n=2-4$.

To understand the basis of our approach, it is important to note that, in principle, the computer resources used by the DMRG method increase linearly with the number of lattice sites (everything else being equal). Therefore, DMRG performances should be better when individual lattice sites are defined so that the number of states n is as small as possible (i.e., $n=2$) even if this implies an increase in the number of sites in the lattice. For instance, in the Hubbard model for fermions, we can either use the same site for both spin up and spin down fermions or use different sites for fermions of different spins. In the first case, the Hilbert space contains $n=4$ states ($|0\rangle,|\uparrow\rangle,|\downarrow\rangle,|\uparrow\downarrow\rangle$) per site. In the second case, the lattice contains twice as many sites but the Hilbert space of each site contains only 2 states ($|0\rangle,|\sigma\rangle$, with $\sigma=\uparrow$ or $\downarrow$). In practice, the second approach is faster by a factor of 2. Also, in a boson-fermion model as the Holstein Hamiltonian (1.1), a site can have both fermion and boson degrees of freedom, or one can separate the boson and fermions into two sites. We have found that the latter method is significantly more efficient than the former. However, it should be kept in mind that DMRG performances depend essentially on the number m of states that one needs to keep per block to obtain a desired accuracy, the number of iterations needed by the DMRG algorithm to converge, and the possible use of system symmetries. All these parameters tend to be unfavorably altered by the partition of sites in smaller units and a large increase of m or of the number of iterations could offset any gain due to the reduction of the Hilbert space dimension. Nevertheless, experience indicates that it is usually possible to improve DMRG performances by substituting several sites with a small Hilbert space for a site with a large Hilbert space.

Therefore, we have developed a method to exactly transform a boson site into several smaller pseudosites. Our approach is motivated by a familiar concept: the representation of a number in binary form. In this case the number is the boson state index starting at 0. Each binary digit is represented by a pseudosite, which can be occupied (1) or empty (0). One can think of these pseudosites as being fermions, but is is simpler to implement them as hard-core bosons, thus avoiding fermion anticommutation minus signs. Thus, for a boson site with $M=2^N$ levels, the level with index 0 is represented by N empty pseudosites, while the highest level, 2^N-1, is represented by N hard-core bosons on the N pseudosites.

To implement this idea, we first choose a truncated occupation-number basis $\{|\alpha\rangle,\alpha=0,1,2,\ldots,2^N-1\}$, where $b^\dagger b|\alpha\rangle=\alpha|\alpha\rangle$, as the finite Hilbert space of a boson site. Then, we introduce N pseudosites $j=1,\ldots,N$ with a two-dimensional Hilbert space $\{|r_j\rangle,r_j=0,1\}$ and the operators $a_j^\dagger,a_j$ such that $a_j|1\rangle=|0\rangle$, $a_j|0\rangle=0$, and $a_j^\dagger$ is the Hermitian conjugate of a_j. These pseudosite operators have the same properties as hard-core boson operators: $a_ja_j^\dagger+a_j^\dagger a_j=1$ and operators on different pseudosites commute. The one-to-one mapping between a boson level $|\alpha\rangle$ and the N-pseudosite state $|r_1,r_2,\ldots,r_N\rangle$ is given by the relation

$$\alpha=\sum_{j=1}^{N}2^{j-1}r_j. \tag{2.1}$$

The next step is to write all boson operators in terms of pseudosite operators. It is obvious that the boson number operator is given by

$$N_b=b^\dagger b=\sum_{j=1}^{N}2^{j-1}a_j^\dagger a_j. \tag{2.2}$$

Unfortunately, other boson operators take a more complicated form in the pseudosite representation. Typically, they are represented by a sum over $\sim M$ terms. They can easily be determined from the definition of the mapping (2.1) and the properties of boson and hard-core boson operators. As an example, we show here how to calculate the representation of $b^\dagger$. First, we write $b^\dagger=B^\dagger\sqrt{N_b+1}$, where $B^\dagger|\alpha\rangle=|\alpha+1\rangle$. The pseudosite operator representation of the second term is

$$\sqrt{N_b+1}=\sum_{\alpha=0}^{M-1}\sqrt{\alpha+1}P_1(r_1)P_2(r_2)\cdots P_N(r_N), \tag{2.3}$$

where $P_j(1)=a_j^\dagger a_j$, $P_j(0)=a_ja_j^\dagger$, and the r_j $(j=1,\ldots,N)$ are given by the mapping (2.1). For $B^\dagger$ we find

$$B^\dagger=a_1^\dagger+a_2^\dagger a_1+a_3^\dagger a_2a_1+\cdots+a_N^\dagger a_{N-1}a_{N-2}\cdots a_1. \tag{2.4}$$

The representation of $b^\dagger$ for any number of pseudosites N is given by the product of these two operators. For instance, for $N=2$ pseudosites,

$$b^\dagger=a_1^\dagger+\sqrt{2}a_2^\dagger a_1+(\sqrt{3}-1)a_1^\dagger a_2^\dagger a_2. \tag{2.5}$$

Other operators can be obtained in a similar way.

We can now substitute $N=\log_2(M)$ pseudosites for each boson site in the lattice and rewrite the system Hamiltonian and other operators in terms of the pseudosite operators. Once this transformation has been done, DMRG algorithms

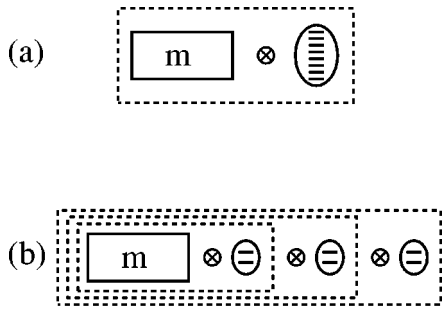

FIG. 1. Symbolic representation of a DMRG step for $N=3$ ($M=8$). In the standard DMRG approach (a), a block (dashed rectangle) is formed by adding a boson site (oval) with its $M=8$ states to the initial block (solid rectangle). In the pseudosite approach (b), a new block is made of the previous block and one pseudosite with 2 states. It takes $N=3$ steps to make the final block (largest dashed rectangle) including the initial block and all pseudosites, which is equivalent to the new block in (a).

can be used to calculate the system properties. For instance, if one would like to find the ground state of an oscillator in a linear potential $H=\omega b^{\dagger}b-\gamma(b^{\dagger}+b)$ keeping $M=4$ states, we would transform this system into a two-site hard-core boson system with the Hamiltonian

$$H=\omega\sum_{j=1}^{2}2^{j-1}a_j^{\dagger}a_j-\gamma[a_1^{\dagger}+\sqrt{2}a_2^{\dagger}a_1+(\sqrt{3}-1)a_1^{\dagger}a_2^{\dagger}a_2+a_1+\sqrt{2}a_1^{\dagger}a_2+(\sqrt{3}-1)a_2^{\dagger}a_2a_1]. \tag{2.6}$$

One can easily check that both Hamiltonians share the same matrix representation in the basis $\{|\alpha\rangle,\alpha=0,1,2,3\}$ and $\{|r_1,r_2\rangle,r_1=0,1,r_2=0,1\}$, respectively.

Figure 1 illustrates the differences between standard and pseudosite DMRG approaches. In the standard approach [Fig. 1(a)], a new block is built up by adding a boson site with M states to another block with m states. Initially, the Hilbert space of the new block contains mM states and is truncated to m states according to the DMRG method. In the pseudosite approach [Fig. 1(b)], we build up a new block by adding one pseudosite with 2 states to another block with m states. The Hilbert space of this new block contains only $2m$ states and is also truncated to m states according to the DMRG method. We have to repeat this step N times until the M-state boson Hilbert space has been added to the original block. However, at each step we have to manipulate only a fraction $2/M$ of the bosonic Hilbert space. It should be noted that the transformation into pseudosites is an exact mapping of truncated bosonic Hilbert spaces. Therefore, the final blocks of both approaches in Fig. 1 would be equivalent if we did not truncate the block Hilbert spaces to m states at each intermediate step. Actually, we have never found any significant differences between pseudosite and standard DMRG results but it is possible that such differences appear when the DMRG truncation error (the error due to the truncation of block Hilbert spaces to m states) is large enough.

Using the transformation into pseudosites we have implemented and tested several DMRG algorithms.[1,2] Generally, implementing a DMRG algorithm for pseudosites is more complicated than a standard DMRG method. This artificial transformation generates a very complicated Hamiltonian, which includes many (typically M) long-range interaction terms between pseudosites. Therefore, at each DMRG step one must keep track of and transform many matrices representing different combinations of pseudosite operators used to build up the Hamiltonian and other operators during following steps. However, one needs the many pseudosite operators only during the intermediate steps of Fig. 1(b). Once the full bosonic Hilbert space has been added to the block [after the final step in Fig. 1(b)], one only needs regular boson operators as in a standard DMRG method. Therefore, in an efficient implementation, matrix representations of boson operators should be computed from the pseudosite operator matrices, which can be discarded after that, whenever it is possible. The cost of this operation ($\propto M$ matrix additions) is small compared to the cost of keeping track of and transforming the pseudosite operator matrices ($\propto M$ matrix multiplications).

III. APPLICATION TO THE HOLSTEIN MODEL

We have applied the pseudosite DMRG method to the Holstein model in different situations: one electron in one and two dimensions, two electrons and half-filled band systems in one dimension, sometimes with additional interactions as an on-site impurity potential or a local electron-electron repulsion (Hubbard term). Although most of the discussion in this section applies to all these different cases, all quantitative results provided here regard the one-electron system with parameters in the range of $0.1\leqslant\omega/t\leqslant 4$, $g<5$.

Several tests have shown that the performance and stability of the DMRG method applied to the Holstein model depend greatly on details of the algorithm used. Below we describe the best approach we have found. We have used the finite system DMRG algorithm[1] to calculate properties of a system of fixed size. However, during the warmup sweep we have not used an infinite system algorithm. Instead, environment blocks are built up using several sites without truncation. With this procedure the accuracy of the results after the warmup sweep is very poor, but this is not a problem because in the finite system algorithm the subsequent iterations (sweeps back and forth across the lattice) can usually make up for a poor quality warmup sweep. The number of states kept per block m is gradually increased as one performs the iterations, and we keep track of the ground-state wave function from step to step to reduce the total calculation time.[2] We have found that it is necessary to optimize the approximate ground state for each intermediate value of m. This optimization requires performing several iterations (up to 6) for each intermediate value of m even if the energy gain brought by these sweeps seems negligible compared to the energy gain, which could be made by increasing m immediately. Otherwise, the DMRG algorithm does not truncate block Hilbert spaces optimally and eventually fails to converge. We think that these additional iterations are needed to optimize the delocalization energy of the electron or polaron, which can be a small fraction of the total energy. The total number of iterations needed by the DMRG algorithm to converge varies greatly and in the worst cases can grow up to 30. Although the Holstein Hamiltonian (1.1) is reflection symmetric, this symmetry has not been used in our algo-

rithm. We have found that using the reflection symmetry can hinder and sometimes prevent the convergence to the ground state.

With the pseudosite DMRG method, we have been able to keep enough states per phonon mode (up to $M=128$) so that the errors from truncation of the phonon basis are negligible. To check that N is large enough, we compute the pseudosite density $A_j=\langle a_j^\dagger a_j\rangle$, where $\langle\rangle$ means the expectation value in the ground state, and extrapolate to find A_{N+1}. N is chosen so that A_{N+1} is comparable to the DMRG truncation error. Usually $N\leqslant 6$ ($M\leqslant 64$) was sufficient.

The polaron problem has an important computational advantage as a test case: the number of states m that need to be kept per block is relatively small. In the noninteracting case ($g=0$), one can easily show that only two eigenstates of the density matrix have a nonzero weight. For finite coupling g, the DMRG truncation error often vanishes (within the machine precision $\approx 10^{-16}$) if we keep a relatively small number of states. Although we need to keep more states when g or the system size increases, we have found that a DMRG truncation error smaller than 10^{-14} can be reached with at most $m=150$ states in all our calculations. This feature has also allowed us to obtain accurate results in quite large two-dimensional systems.

With the DMRG method, the error on the ground-state energy is generally proportional to the DMRG truncation error. Therefore, we can calculate the ground-state energy and the truncation error for several values of m and use a linear fit to extrapolate the result without truncation error.[1] This method gives reliable estimations of the error on the ground state energy. In one dimension we have obtained relative errors in the range of 10^{-10}–10^{-16} depending on the system size and parameters g, ω/t. In two dimensions we have contented ourself with larger errors, from 10^{-6} to 10^{-10}, to save CPU time but more accurate results can be obtained.

In the polaronic regime, the density of states near the ground state becomes very large (see the discussion in Sec. V). Thus, a small energy error does not guarantee that we have obtained an accurate ground-state wave function. To estimate the precision of measurements $\langle O\rangle$, where O is any operator other than the Hamiltonian H, we have used exact relations between expectation values, such as symmetry conditions or self-consistence equations. For instance, the self-consistence equation

$$\langle b_\diagup^\dagger + b_\diagup\rangle = 2g\langle n_\diagup\rangle, \tag{3.1}$$

which holds for all eigenvalues of the Holstein Hamiltonian (1.1), gives a local condition on both fermion and boson degrees of freedom. For the results presented in this paper we have typically obtained relative errors smaller than 10^{-4} in one dimension and smaller than 10^{-2} in two dimensions. Finally, we point out that the pseudosite DMRG method perfectly reproduces exact diagonalization results for the ground state and lowest excited states of small systems like the two-site Holstein model.[10]

For each value of the parameters g and w/t we have studied systems of different sizes and checked that finite-size effects are negligible or extrapolated results to an infinite system. The largest system sizes that we have used to study the one-dimensional Holstein model are $L=80$ sites for $N\leqslant 5$ ($M\leqslant 32$) and $L=30$ sites for $5<N\leqslant 7$ ($32<M\leqslant 128$). In two dimensions, we have used square lattices with up to 20×20 sites for $N\leqslant 3$ ($M\leqslant 8$) and up to 12×12 sites for $4<N\leqslant 6$ ($16<M\leqslant 64$). In most cases we could easily study much larger lattices if we needed to. However, in the polaronic regime, the largest system size for which we can compute the ground state accurately is limited by the finite precision of the DMRG method. We will discuss this point further in Sec. V.

The relatively small number of states needed for the polaron problem allows us to carry out some calculations with both the standard and pseudosite approaches and to compare their performances in terms of CPU time and memory storage. In test calculations with all parameters equal, we have found that performances of both approaches are similar for small M but the pseudosite approach becomes better for $M\geqslant 8$. The differences between these methods increase very rapidly with M, as expected, and, more surprisingly, with m. For $M=32$ and $m=50$, the pseudosite approach requires only 1/8 of the memory used by the standard approach and is faster by two orders of magnitude. In real applications, however, we expect the performance difference between both approaches to be smaller because of the greatest flexibility and simplicity of a standard approach. For instance, M can take any integer value in the standard approach. Nevertheless, when computations become challenging (for $M\geqslant 16$ and $m\geqslant 50$), the pseudosite approach clearly outperforms the standard approach.

IV. RESULTS

Using the numerical method presented in the previous sections, we have studied the ground-state properties of the Holstein Hamiltonian (1.1) with a single electron in one and two dimensions. In particular, we are interested in the evolution of the ground state as a function of the adiabaticity ω/t and of the electron-phonon coupling g. For a weak coupling a standard perturbation calculation in g shows that the ground state is a quasi-free-electron dragging a phonon cloud, which slightly renormalizes the electron effective mass. Note that the weak-coupling regime roughly corresponds to $g<1$ and $2g^2\omega<W$, where $W=4t$ in one dimension and $W=8t$ in two dimensions is the bare electronic bandwidth. The standard strong-coupling theory of the Holstein model,[16] which is based on the Lang-Firsov transformation and treats the electron hopping term as a perturbation, predicts a polaronic ground state with a narrow bandwidth. The strong-coupling regime corresponds to $g>1$ and $2g^2\omega>W$. In this section, we present several results of pseudosite DMRG calculations which show the evolution of the ground states from the weak to the strong electron-phonon coupling regime and compare them to the predictions of perturbation calculations and the results of previous numerical studies.

A. Electronic density

For periodic boundary conditions, it is known rigorously that the ground-state energy and wave function are analytic functions of the electron-phonon coupling g.[17] In particular,

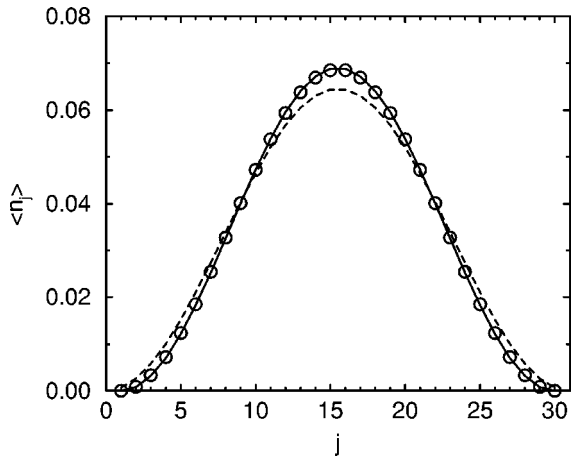

FIG. 2. Ground-state density distribution for $\omega=t$, $g=2.5$ in a 30-site chain. The solid and dashed curves are given by Eq. (4.1) with $a=1$ and 0, respectively.

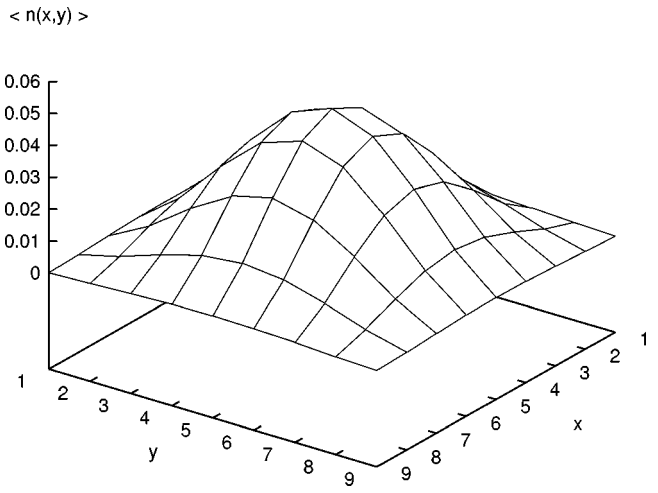

FIG. 3. Ground-state density distribution for $\omega=t$, $g=2.2$ on a 9×9 lattice.

no phonon-induced localization transition (breaking of the translation symmetry) occurs for finite g; in the ground state the electron is always delocalized over the lattice. Correspondingly, for open chains our DMRG results show that the electronic density $\langle n_\ell \rangle$ always has the shape

$$n(\ell)=\frac{2}{L+1-2a}\sin^2\left(\frac{\pi(\ell-a)}{L+1-2a}\right) \tag{4.1}$$

for $1+a\leq\ell\leq L-a$ and $n(\ell)=0$ otherwise, where a is an integer number. This density corresponds to a free particle in a one-dimensional box made of the sites with indices $\ell=1+a$ to $\ell=L-a$. Therefore, the electron is delocalized over the whole lattice, except for some chain edge effects, in qualitative agreement with the exact result for periodic boundary conditions. For small coupling g, we have found that we obtain the best fit with $a=0$ as for a free electron. For stronger couplings better fits can be obtained with larger values of a. For instance, Fig. 2 shows a density obtained with the DMRG method and the function (4.1) for $a=0$ and 1. Even when the best fit is obtained with $a>0$, the density $\langle n_\ell \rangle$ close to the chain edges is actually finite but very small.

On two-dimensional square lattices the electron is also delocalized over the lattice for all values of the parameters g and ω/t that we have investigated. For instance, in Fig. 3, we show the density $\langle n_{x,y} \rangle$ for a lattice in the strong-coupling regime. In the weak-coupling regime, the electronic density distribution has the same shape

$$n(x,y)=\frac{4}{(L+1)^2}\sin^2\left(\frac{\pi x}{L+1}\right)\sin^2\left(\frac{\pi y}{L+1}\right) \tag{4.2}$$

as the density of a free particle in a two-dimensional box. As in one dimension, for stronger coupling the density becomes larger in the middle of the lattice and decreases near the edges, but in this case we cannot fit the density $\langle n_{x,y} \rangle$ with Eq. (4.2) and a renormalized system size.

B. Electron-lattice correlations

Some ground-state properties can easily be studied in terms of static correlation functions $\langle n_i q_j \rangle$ between the electron position and the oscillator displacement $q_j=b_j^\dagger+b_j$. These correlations indicate the strength (for $i=j$) of the electron-induced lattice deformation and its spatial extent. In the noninteracting case ($g=0$) they are uniformly zero. Figure 4 shows the normalized correlation functions $\chi_{10,j}=\langle n_{10}q_j\rangle/\langle n_{10}\rangle$ for several parameters ω/t and g in 20-site chains. For parameters close to the weak-coupling regime [Figs. 4(a) and 4(c)] the amplitude of $\chi_{10,j}$ is smaller than the quantum lattice fluctuations, which are given by the zero-point fluctuations of each phonon mode $\sigma_q\approx1$. Therefore, these correlations do not show a lattice deformation that could trap an electron because the sign of the effective lattice potential seen by the electron fluctuates. They are merely the signature of a phonon cloud following the electron. For parameters close to the strong-coupling regime [Figs. 4(b) and 4(d)], the amplitude of $\chi_{10,j}$ is larger than these quantum lattice fluctuations. In these cases, we really observe a lattice deformation generating a local attractive potential that is likely to trap the electron.

We observe similar features in two-dimensional lattices. Figure 5 shows a normalized correlation function $\chi(x,y)=\langle n_{8,8}q_{x,y}\rangle/\langle n_{8,8}\rangle$ in the weak-coupling regime. The amplitude of $\chi(x,y)$ is much smaller than quantum lattice fluctuations $\sigma_q\approx1$. In Fig. 6 we show a similar correlation function, $\chi(x,y)=\langle n_{5,5}q_{x,y}\rangle/\langle n_{5,5}\rangle$, in the strong-coupling regime. In this case the amplitude of the lattice deformation generated by the electron is clearly larger than the zero-point lattice fluctuations.

In the weak-coupling limit we observe an exponential decay of correlations between electron position and lattice deformation. We find good agreement between our DMRG results and weak-coupling perturbation results for all phonon frequencies ω/t, even in the nonadiabatic regime ($\omega/t>1$) where the correlations decrease very fast. In the adiabatic ($\omega/t<<1$) weak-coupling limit, the lattice deformation extends over many sites [Fig. 4(a)]. When g or ω/t increases, the spatial extent of the lattice deformation decreases. In the strong-coupling limit, the ground state becomes ''superlocalized'' in the sense that any operator measuring a correlation between the electron and a phonon vanishes unless the correlation is measured on the same site.[8] In particular, one finds $\langle n_i q_j \rangle\sim\delta_{ij}$ [see Fig. 4(d) and Fig. 6]. The variation of

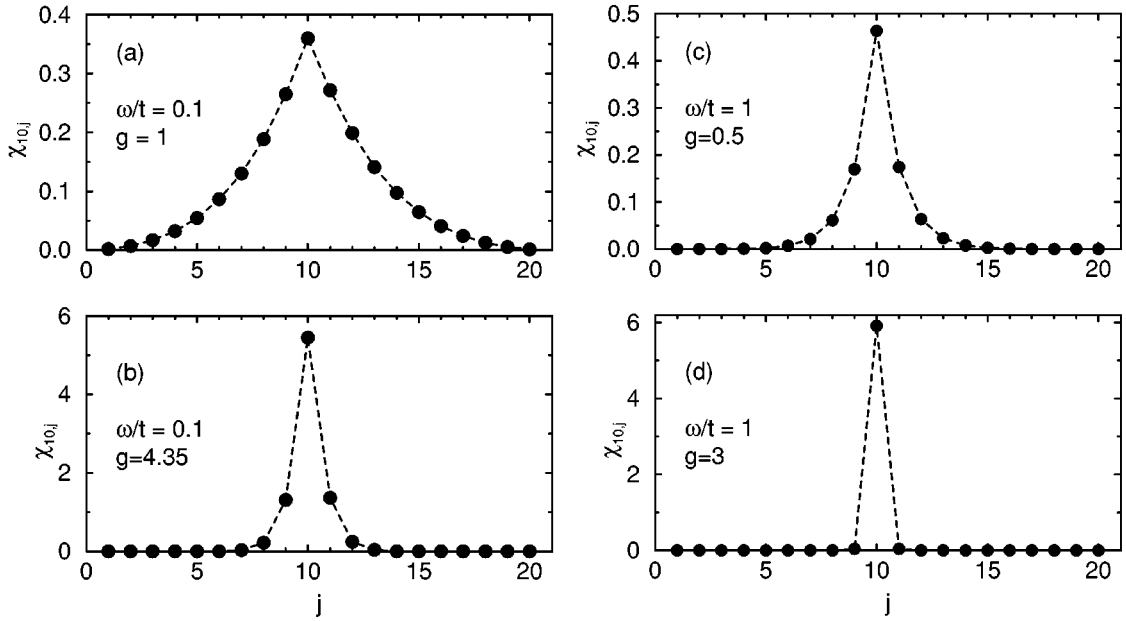

FIG. 4. Correlations $\chi_{10,j}$ between electron density and lattice displacements on 20-site chains for various values of ω/t and g.

the lattice deformation extent as a function of ω/t can easily be understood as a retardation effect. For small ω/t, phonons are much slower than the electron and thus phonon modes that are excited by the passage of the electron take a long time to relax. Therefore, we can observe a lattice deformation far away from the current position of the electron. In the antiadiabatic limit ($\omega/t \gg 1$), lattice fluctuations are fast and a lattice deformation relaxes quickly following the slow electronic motion. Thus, we can observe a lattice deformation only in the vicinity of the electron.

It should be kept in mind that these correlations only show expectation values of the lattice displacements q_ℓ with respect to an instantaneous electron position. They do not show the electron density distribution for a specific frozen lattice configuration. Therefore, these results alone are not evidence for the formation of a self-trapped electronic state and they give no information regarding the electron density distribution within a polaron. To obtain this information we should compute $\langle P_i n_j \rangle$, where P_i projects the phonon states onto a particular lattice configuration representing a polaron centered on site i. Unfortunately, we do not know the operator P_i.

C. Self-trapping crossover

Previous numerical studies have shown that there is a critical value of the electron-phonon coupling above which self-trapping of the electron by a local lattice distortion does occur.[8,10,13,14] One should keep in mind that no localization of the ground-state wave function is involved in self-trapping. Therefore, a smooth crossover from a quasi-free-electron ground state to a polaronic ground state does not contradict rigorous results on the absence of localization in this kind of model.[17] Moreover, self-trapping does not imply any change in the electronic density distribution. If the elec-

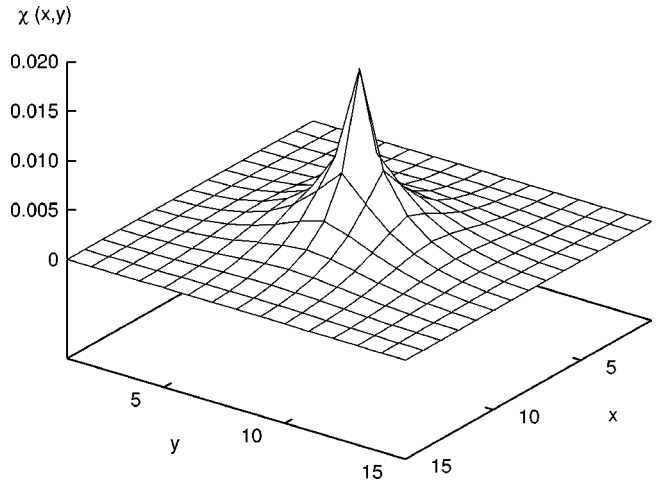

FIG. 5. Correlations $\chi(x,y)$ (see text) between electron position and lattice deformation on a 15×15 lattice with $\omega=0.2t$ and $g=0.1$. The electron position is on the center of the lattice.

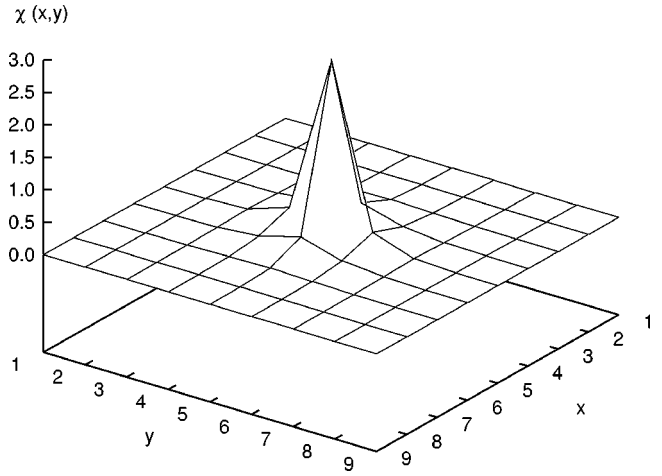

FIG. 6. Correlations $\chi(x,y)$ (see text) between electron position and lattice deformation on a 9×9 lattice with $\omega=t$ and $g=2.2$. The electron position is on the center of the lattice.

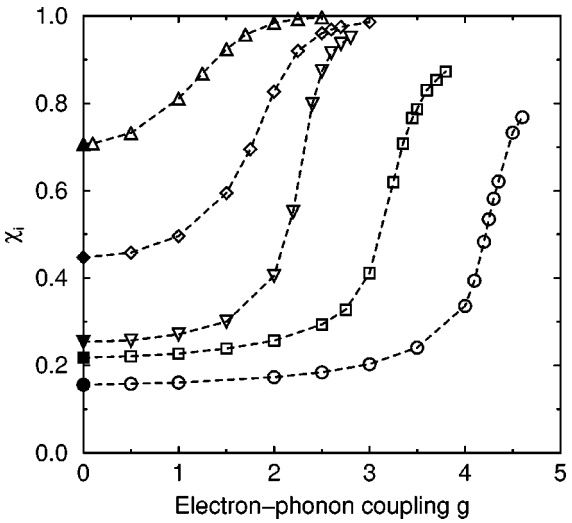

FIG. 7. Local electron-lattice correlation χ_i as a function of the electron-phonon coupling g for $\omega/t=0.1$ (circle), 0.2 (square), 1 (diamond), and 4 (up triangle) in one dimension and for $\omega/t=1$ (down triangle) in two dimensions. Open symbols are DMRG results. Filled symbols show first-order weak-coupling perturbation results.

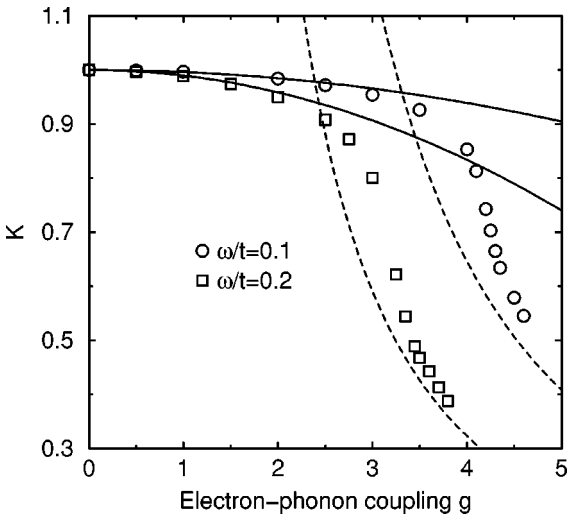

FIG. 8. Electronic kinetic energy as a function of the electron-phonon coupling g in one-dimensional systems in the adiabatic regime. Symbols are DMRG results. Solid curves show the second-order weak-coupling perturbation results. Dashed curves are the predictions of the second-order strong-coupling expansion.

tron is self-trapped by a local lattice deformation, the resulting polaron is delocalized over the lattice and the polaron appears only in correlations between electron and lattice.

A measure of the polaronic character of the electron is the correlation function

$$\chi_i=\frac{\langle n_i q_i\rangle}{2g\langle n_i\rangle}, \tag{4.3}$$

where the index i is either a site index ℓ on a chain or (x,y) on a square lattice. Using Eq. (3.1), one can also write $\chi_i=\langle n_i q_i\rangle/\langle q_i\rangle$. Therefore, it is clear that $|\chi_i|\leqslant 1$. In practice, we have found that χ_i takes only a positive value between 0 and 1. For periodic boundary conditions, this function is constant and differs from the function $\chi_{i,0}$ described in Ref. 14 only by a factor of $L/2g$ ($L^2/2g$ in two dimensions). In open systems, the term $\langle n_i\rangle$ in the denominator is needed to compensate for the inhomogeneous density distribution. We have found that this function is almost constant, except close to the lattice edges. Here we report and discuss only values of χ_i obtained in the central region of a lattice.

In Fig. 7 we show our DMRG results for χ_i as a function of the electron-phonon coupling g for different values of ω/t. For small coupling g our results tend to the value predicted by the weak-coupling perturbation theory. For larger coupling, χ_i tends to 1 as predicted by strong-coupling theory. At intermediate coupling, one observes a rather sharp, though continuous, transition from the weak-coupling to the strong-coupling value of χ_i as g increases. We think that this transition marks the crossover from a quasi-free-electron ground state to a polaronic ground state. The crossover roughly occurs when both conditions $g>1$ and $g^2\omega \geqslant W/2$ are fulfilled, in agreement with previous works.[10,13,14] However, since the formation of polaron does not break any symmetry and all ground-state properties are analytic functions of the parameters, it is impossible to define critical values g_c and ω_c separating quasi-free-electron and polaronic regimes. Unlike Capone *et al.*,[14] we have found that the crossover is always marked by a sharp increase of χ_i in a small region of the plane $(g,\omega/t)$, even for large ω/t. The problem is that these authors have not normalized their function $\chi_{i,0}$ by a factor g as we do in Eq. (4.3). Therefore, they observe a quasilinear dependence as a function of the electron-phonon coupling g, which hides the sharp but small increase that we observe in Fig. 7 at large phonon frequencies.

In two dimensions χ_i is smaller than in one dimension for the same parameters g and ω/t. The crossover occurs at stronger coupling because the bandwidth W is larger in higher dimension and thus the condition $2g^2\omega>W$ is fulfilled for larger g. However, differences between χ_i for one- and two-dimensional systems diminish when the coupling increases (see results for $\omega=t$ in Fig. 7).

D. Electronic kinetic energy

One can obtain some insight about the electron state by calculating its kinetic energy (in units of the kinetic energy at $g=0$)

$$K=\frac{2t}{W}\sum_{\langle \ell,m\rangle}\langle c_m^\dagger c_\ell + c_\ell^\dagger c_m\rangle. \tag{4.4}$$

Figures 8 and 9 show the evolution of the kinetic energy K as a function of the electron-phonon coupling g in the adiabatic and nonadiabatic regime, respectively. These results are qualitatively similar to recent exact diagonalization results on small lattices.[13] For weak coupling, K is very close to 1. This means that the electron is barely affected by the interaction with the phonons and remains essentially in the same state as a free electron. Further evidence for a quasi-free-electron ground state is the good agreement between our DMRG results and the second-order perturbation calculation in g, at least as long as $g^2\omega<W/2$ or $g<1$. Therefore, we think that the electron is not trapped by any lattice deforma-

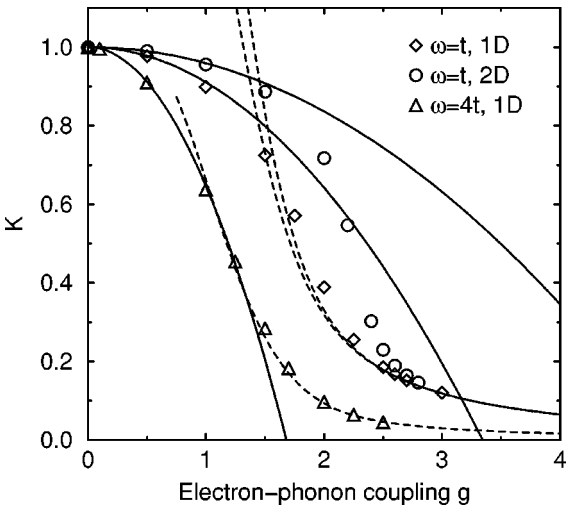

FIG. 9. Electronic kinetic energy as a function of the electron-phonon coupling g in one-dimensional (1D) and two-dimensional (2D) systems in the nonadiabatic regime. Symbols are DMRG results. Solid curves show the second-order weak-coupling perturbation results. Dashed curves are the predictions of the second-order strong-coupling expansion.

tion in this regime but simply drags a phonon cloud. We also note that for $\omega/t=t$ and $g=0.5$, static correlations $\langle n_i q_j \rangle$ decay over a few sites [see Fig. 4(c)] while we find $K \approx 0.977$, which is not compatible with an electron localized on a few sites. This confirms that the spatial extent of lattice deformation obtained from $\langle n_i q_j \rangle$ can be different from the localization length of the electron around a lattice distortion.

In the crossover region the kinetic energy decreases rapidly with increasing coupling. For large enough g our DMRG results tend to the values predicted by the second-order strong-coupling theory. The agreement between these results is better for larger values of ω/t because the strong-coupling theory is a perturbative expansion in $t/(g^2\omega)$ and thus much more accurate in the antiadiabatic limit. Also, our results confirm that the first-order strong-coupling method, which predicts $K \sim \exp(-g^2)$, is a very poor approximation for all values of ω/t. It is necessary to include at least the second-order term in t in the perturbative expansion to obtain reliable results.

In Fig. 9 we can see that initially K decreases faster in one dimension than in two dimensions for similar parameters. Nevertheless, for large coupling g, our numerical results and the strong-coupling theory show that K converges to the same values $\sim t/(g^2\omega)$ in both dimensions.

Finally, we note that for $\omega=4t$ (see Fig. 9), the combination of second-order weak- and strong-coupling theory can reproduce our numerical results for all values of g very accurately. Therefore, these methods seem sufficiently accurate to study the polaron problem in the antiadiabatic limit and could be very useful in cases where numerical methods are not practical, for instance, in higher dimensions. However, one should keep in mind that the strong-coupling theory gives poor results in the crossover regime for smaller values of ω/t.

V. EFFECTIVE MASS

A polaron or a quasi-free electron with its phonon cloud can be seen as an itinerant quasi-particle if its effective bandwidth exceeds perturbations of its formation energy by external forces. Therefore, it is interesting to compute parameters that describe its dynamics, such as its effective mass $m^\star$.

The electronic density distribution shows that the electron or polaron is delocalized over the lattice as a free particle. We know that the band structure of a free particle in an open chain of length L would be given by $E(k)=-2t^\star\cos(k)$ with $k=z\pi/(L+1)$, where $z=1,2,3,\ldots$ numbers the eigenstates. The effective hopping term $t^\star$ is related to the effective mass by $m^\star/m=t/t^\star$, where m is the bare electron mass. However, the polaron band structure is known to deviate from this form because of the importance of effective long-range hopping terms.[13,15] Nevertheless, for large chains ($L \gg 1$) we expect the electronic excitation spectrum at low energy to be given by

$$E(z,L)=E_\infty+t^\star\left(\frac{z\pi}{L+1-2a}\right)^2, \tag{5.1}$$

where E_∞ is the ground state energy of an infinite chain and a is a parameter that accounts for the reduction of the effective system length due to the repulsive effect of the chain edge. We can determine the parameters E_∞, $t^\star$, and a by calculating different eigenenergies $E(z,L)$ with the DMRG and then fitting these results to Eq. (5.1). In principle, we should vary z in this equation and thus calculate the ground state and several excited states. However, calculating accurate excitation energies with the DMRG is much more difficult than computing ground-state energies. Moreover, the task of computing electronic excited states is complicated by the intrusion of phononic excitations in the spectrum. Therefore, we have obtained effective masses by fitting ground-state energies for several chain lengths L to Eq. (5.1) with $z=1$. This method only yields the effective mass at the bottom of the electronic or polaronic band but in this particular case gives results similar to those obtained by fitting excited-state energies. We generally obtain excellent fit with this method as soon as $L+1-2a>10$. We estimate that the error on our values for $m^\star$ is a few percent or smaller. The value of a that gives the best fit of the energy to Eq. (5.1) is generally close to the value of a that reproduces the density distribution in Eq. (4.1). Therefore, the behavior of the ground-state energy as a function of the system size confirms that the electron or polaron behaves like a free particle on a chain of effective length $L-2a$ for all values of the parameters g and ω/t.

In two dimensions we use a similar procedure. The ground-state energy for several square lattices of size $L\times L$ is fitted to Eq. (5.1) with $z=1$ and $2t^\star$ substituted for $t^\star$. The linear dimensions L used in these calculations were generally smaller than the chain lengths used in one-dimensional systems. Thus, the mass obtained for two-dimensional systems is less accurate and we estimate that the relative error is $\leqslant 20\%$.

The structure (5.1) of the electronic excitation spectrum allows us to understand the main difficulty in applying the DMRG method to the polaron problem. To determine the ground state accurately, we need an absolute precision that is better than the energy difference between the first excited state ($z=2$) and the ground state ($z=1$). Therefore, the relative error on the ground-state energy must be smaller than

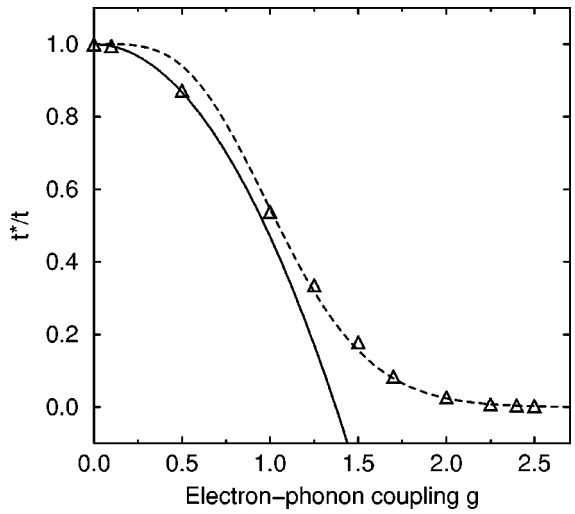

FIG. 10. Effective hopping integral t^* as a function of the electron-phonon coupling g for $\omega/t=4$ in one dimension. Symbols are DMRG results. The solid curve is the second-order weak-coupling perturbation result. The dashed curve shows the second-order strong-coupling expansion prediction.

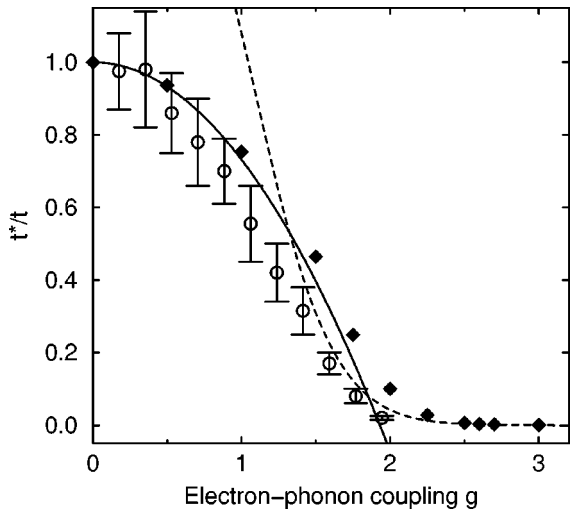

FIG. 11. Effective hopping integral t^* as a function of the electron-phonon coupling g for $\omega/t=1$ in one dimension. Diamonds are DMRG results. The solid curve is the second order weak-coupling perturbation result. The dashed curve shows the second-order strong-coupling expansion prediction. Circles with error bars are QMC results.

$\sim t^\star/(E_\infty L^2)$. As the precision of our numerical method is limited by roundoff errors, this condition imposes a constraint on the parameters g, ω/t, and L for which we can find the ground state. Using the strong-coupling theory results,[16] one can easily show that for $g\to\infty$, $E_\infty\to -g^2\omega$, and $t^\star \to t\exp(-g^2)$. Therefore, the minimal precision that we need goes as $\sim t\exp(-g^2)/(L^2g^2\omega)$ and becomes exceedingly small very rapidly with g. In practice, we have been able to obtain the ground state of chains with up to $L=16$ sites for very heavy polarons ($t^\star/t\approx 10^{-4}$). Calculating the effective hopping accurately with Eq. (5.1) requires a higher precision and thus is limited to a smaller set of parameters. We can measure the effective hopping with a good accuracy for $t^\star \geqslant 10^{-3}t$ using chains with up to $L=30$ sites or square lattices with up to 10×10 sites at least. In this paper we report results for the effective mass (or hopping) in this range only. Of course, in the quasi-free-electron and crossover regimes, where $t^\star\sim t$ and $E_\infty \leqslant 2t$ this problem is less serious and we can study much larger systems.

In Fig. 10 we show the effective hopping $t^\star$ calculated with our DMRG method as well as the second-order weak- and strong-coupling results for $\omega/t=4$ in one dimension. The good agreement between these results confirms both the accuracy of perturbative methods in the antiadiabatic limit and the validity of our method. We have found that our DMRG results also agree well with the weak-coupling results in the quasi-free-electron regime for all values of ω/t. However, as ω/t decreases, we observe differences between our results and the strong-coupling theory, which becomes more and more important. The ratio between the values of $t^\star$ obtained with the DMRG and the strong-coupling theory increases rapidly and can reach 10^5 for $\omega/t=0.1$. We think that this discrepancy is due to the limitation of the strong-coupling theory, which is a perturbative expansion in $t/(g^2\omega)$ and thus becomes inaccurate for small ω/t.

In Fig. 11 we show the same results for $\omega/t=1$ together with the effective hopping obtained by a new quantum Monte Carlo (QMC) calculation.[9] There is qualitative agreement between DMRG and QMC results but our values of $t^\star$ are always larger than those obtained by QMC calculations. We can see that the DMRG method is more accurate than the QMC method at weak coupling. We also note that QMC results are systematically lower than the strong-coupling predictions. On the other hand, we have found that DMRG results are always larger than these strong-coupling predictions. It is known that the second-order strong-coupling perturbation theory underestimates the effective bandwidth for large coupling.[15] Therefore, we think that this new QMC method underestimates the effective hopping in the ground state of the Holstein model.

Finally, we show the effective mass $m^\star$ as a function of the electron-phonon coupling in Fig. 12. At finite coupling the quasi-free-electron or polaron effective mass is larger

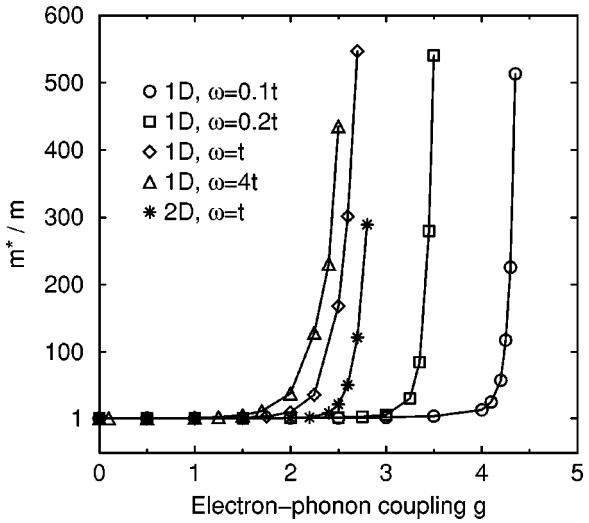

FIG. 12. Effective mass of the electron or polaron as a function of the electron-phonon coupling g for different values of ω/t in one-dimensional (1D) and two-dimensional (2D) systems.

than the bare electron mass because of the phonon cloud that must be dragged by the electron. The sudden onset of self-trapping is marked by an abrupt increase of the effective mass. However, the effective mass that we calculate is a ground-state property and its dependence on coupling constants is smooth, in agreement with exact theorems on the ground state of the Holstein model.[17] In the polaronic regime, the effective mass increases exponentially with the coupling, but in the adiabatic regime $\omega \leqslant t$ the mass enhancement is significantly smaller than the prediction of the first-order strong-coupling theory, $m^{\star}/m = \exp(-g^2)$, as noted previously.[13,15] The evolution of $m^{\star}$ is similar in one and two dimensions. The only difference is the shift of the crossover regime to a larger value of g due to the variation of the bare electronic bandwidth W as discussed in the previous section.

As all ground-state results are smooth at the self-trapping transition we cannot determine precisely when a quasi-free-electron becomes a polaron. It is necessary to study excited states or dynamical properties to find qualitative differences between both regimes.[10,13] Nevertheless, our results show that for some parameters, for instance, $\omega = t$ and $g \approx 2-2.2$, the ground state is clearly a polaron and the effective mass is relatively small, $m^{\star}/m \approx 10-100$. Therefore, in the Holstein model there are polarons with an effective mass that is much smaller than the prediction of the standard small polaron theory.[6]

VI. CONCLUSION

In this paper we have presented a DMRG approach to study lattice systems including bosonic degrees of freedom. The pseudosite DMRG method is much more efficient than a standard approach using regular boson sites and allows us to study large systems while keeping up to 128 states in each bosonic Hilbert space. We have successfully applied this method to the Holstein model and we believe that it can be applied to any model including boson, which can be studied with a standard DMRG method. A specific feature of the Holstein model is the absence of direct interaction terms between bosons on different sites. In models including such terms,[3,5] one expects a decrease of the pseudosite DMRG performances because of the introduction of additional long-range interactions between pseudosites. Nevertheless, a pseudosite approach is likely to be more efficient than the standard approach even in this case.

The pseudosite DMRG is just a method that efficiently handles the large number of states of a boson site. A better approach would be to reduce the number of states one needs to represent a boson site using the key idea of DMRG. In such an approach the reduced density matrix for a single site is diagonalized to obtain a small set of optimized states representing the boson site. It has been shown that 3 optimized states per site give results as accurate as with 10–100 states in exact diagonalizations of the one-dimensional Holstein model at half-filling.[18] Coupling this approach to the DMRG will further improve our capability to perform numerical studies of systems including bosonic degrees of freedom.

Using the pseudosite DMRG method, we have studied the ground state of the one- and two-dimensional Holstein model with a single electron. We have been able to study all regimes of parameters g and ω/t in systems large enough to eliminate finite-size effects. Our results are in good agreement with exact theorems, perturbation theory predictions, and the results of previous numerical works. We have not found any qualitative differences between the one- and two-dimensional systems after taking into account the doubling of the bandwidth in two dimensions compared to one dimension.[15] In particular, in the weak-coupling regime self-trapping does not occur and the ground state is a quasi-free-electron in both one and two dimensions.[8] Several ground-state properties show a smooth but quite abrupt crossover from a quasi-free-electron to a polaronic ground state as the electron-phonon coupling increases. In particular, the crossover is signaled by a sharp increase of the effective mass, although the mass enhancement can be much smaller than predicted by the standard small polaron theory.

ACKNOWLEDGMENTS

We wish to acknowledge the support of the Campus Laboratory Collaborations Program of the University of California. We acknowledge support from the NSF under Grant No. DMR-9509945, and from the San Diego Supercomputer Center. E.J. thanks the Swiss National Science Foundation for financial support.

[1] S. R. White, Phys. Rev. Lett. **69**, 2863 (1992); Phys. Rev. B **48**, 10 345 (1993).
[2] S.R. White, Phys. Rev. Lett. **77**, 3633 (1996).
[3] R.V. Pai, R. Pandit, H.R. Krishnamurthy, and S. Ramasesha, Phys. Rev. Lett. **76**, 2937 (1996).
[4] L.G. Caron and S. Moukouri, Phys. Rev. Lett. **76**, 4050 (1996).
[5] L.G. Caron and S. Moukouri, Phys. Rev. B **56**, 8471 (1997).
[6] T. Holstein, Ann. Phys. (N.Y.) **8**, 325 (1959); **8**, 343 (1959).
[7] H.B. Shore and L.M. Sander, Phys. Rev. B **7**, 4537 (1973); A. LaMagna and R. Pucci, *ibid.* **53**, 8449 (1996); D. W. Brown, K. Lindenberg, and Y. Zhao, J. Chem. Phys. **107**, 3179 (1997).
[8] H. De Raedt and A. Lagendijk, Phys. Rev. B **27**, 6097 (1983); **30**, 1671 (1984).
[9] P.E. Kornilovitch and E.R. Pike, Phys. Rev. B **55**, 8634 (1997).
[10] J. Ranninger and U. Thibblin, Phys. Rev. B **45**, 7730 (1992); E.V.L. de Mello and J. Ranninger, *ibid.* **55**, 14 872 (1997).
[11] A.S. Alexandrov, V.V. Kabanov, and D.K. Ray, Phys. Rev. B **49**, 9915 (1994).
[12] F. Marsiglio, Physica C **244**, 21 (1995).
[13] G. Wellein, H. Röder, and H. Fehske, Phys. Rev. B **53**, 9666 (1996); G. Wellein and H. Fehske, Phys. Rev. B **56**, 4513 (1997); H. Fehske, J. Loos, and G. Wellein, e-print cond-mat/9709011(1997).
[14] M. Capone, W. Stephan, and M. Grilli, Phys. Rev. B **56**, 4484 (1997).
[15] W. Stephan, Phys. Rev. B **54**, 8981 (1996).
[16] J.E. Hirsch and E. Fradkin, Phys. Rev. B **27**, 4302 (1983).
[17] B. Gerlach and H. Löwen, Rev. Mod. Phys. **63**, 63 (1991).
[18] C. Zhang, E. Jeckelmann, and S.R. White, e-print cond-mat/9709187(1997).